A Robust Multibit Multiplicative Watermark Decoder Using a Vector-Based Hidden Markov Model in Wavelet Domain

Marzieh Amini, *Student Member, IEEE*, M. Omair Ahmad, *Fellow, IEEE*, and M.N.S. Swamy, *Fellow, IEEE*

***Abstract*— The vector-based hidden Markov model (HMM) is a powerful statistical model for characterizing the distribution of the wavelet coefficients, since it is capable of capturing the subband marginal distribution as well as the inter-scale and cross-orientation dependencies of the wavelet coefficients. In this paper we propose a scheme for designing a blind multibit watermark decoder incorporating the vector-based HMM in wavelet domain. The decoder is designed based on the maximum likelihood criterion. A closed-form expression is derived for the bit error rate and validated experimentally with Monte Carlo simulations. The performance of the proposed watermark detector is evaluated using a set of standard test images and shown to outperform the decoders designed based on the Cauchy or generalized Gaussian distributions without or with attacks. It is also shown that the proposed decoder is more robust against various kinds of attacks compared with the state-of-the-art methods.**

***Index Terms*— Hidden Markov model (HMM), image watermarking, optimum watermark decoder, wavelet transform.**

I. Introduction

DIGITAL watermarking is a technique for data hiding whereby a message is embedded in the host signal for the protection of illegal duplication and distribution of multimedia data. Image watermarking algorithms can be classified into two categories depending on the domain used for embedding the watermark, spatial [1] or frequency [2]–[28]. Frequency-domain methods, such as those based on discrete Fourier transform (DFT) [2]–[4], discrete cosine transform (DCT) [5]–[7], digital wavelet transform (DWT) [8]–[24], ridgelet transform [25], [26], and contourlet transform [14], [27], [28], have been commonly used in recent works. There are several methods of embedding the watermark: additive [5]–[12], [18], [21]–[25], multiplicative [3], [4], [13], [14], [19], [27]–[30], [32], scaling [17], [26], and quantization [15], [33].

In some applications of watermarking, it may only be necessary to determine whether a specific watermark is present or not in the received signal [3], [5]–[13], [21], [27], [29], [30], [32], whereas in the others, the embedded watermark is considered as a hidden unknown message that needs to be decoded accurately [4], [5], [14]–[17], [19], [22]–[24], [25], [26], [28], [31], [33], [41], [42]. In order to implement a blind watermark detector or decoder, the statistical properties of the image are commonly used. Therefore, efforts in this direction have been mostly on the statistical modeling of the transform domain coefficients [4]–[14], [21]–[24], [26]–[30], [32]. There exist several works focusing on watermark decoding using the statistical properties of the transformed domain coefficients. In [5], additive watermarking has been performed in the DCT domain, and decoding has been performed by using the generalized Gaussian (GG) distribution as a prior model for the DCT coefficients. In [4], an optimum decoder for a multiplicative watermark has been proposed in the DFT domain using the Weibull distribution in which the performance of the decoder has been evaluated by Monte Carlo simulations. In [17], a scaling-based watermarking in the wavelet domain has been proposed by assuming a Gaussian distribution for modeling the wavelet coefficients. In [32], a multiplicative watermarking has been proposed in the contourlet domain using the GG distribution. In [19], a multiplicative watermarking decoder has been proposed for fingerprint application in the wavelet domain using the GG distribution. In [16], a quantization-based method has been proposed in the logarithmic domain. In [15], a quantization-based image watermarking has been proposed in which the watermark bits are embedded by quantizing the angles of significant gradient vectors in the wavelet domain. Among all the transforms employed, the wavelet transform has received the greatest attention due to its multiresolution and compression properties. Even though the wavelet coefficients of an image within and across the scales have strong dependencies, most of the previous works on the watermark detection and decoding have assumed these coefficients to be independent and modeled them by marginal distributions, such as the Gaussian [7], Gauss–Hermite [8], GG [5], [19], Cauchy [6], and Bessel-K form [9]. On the other hand, the joint statistical models, such as the Markov random field priors [35] and the hidden Markov model (HMM) [36] that successfully capture these dependencies, have also been proposed. However, in [37], a two-state vector-based HMM has been proposed that captures not only the inter-scale dependencies, but also the cross-orientation dependencies of the wavelet coefficients. In [11], [12], [38], and [39], it has

Manuscript received November 4, 2015; revised July 15, 2016; accepted August 23, 2016. Date of publication September 8, 2016; date of current version February 13, 2018. This work was supported in part by the Natural Sciences and Engineering Research Council of Canada and in part by the Regroupement Strategique en Microelectronique du Quebec. This paper was recommended by Associate Editor P. Salama. *(Corresponding author: M. Omair Ahmad.)*

The authors are with the Center for Signal Processing and Communications, Concordia University, Montreal, QC H3G 1M8, Canada (e-mail: ma_amini@encs.concordia.ca; omair@encs.concordia.ca; swamy@encs.concordia.ca).

Color versions of one or more of the figures in this paper are available online at http://ieeexplore.ieee.org.

Digital Object Identifier 10.1109/TCSVT.2016.2607299

been shown that the M-state vector-based HMM distribution provides a fit that is very close to the distribution of the wavelet coefficients of images, as measured in terms of the Kolmogorov–Smirnov distance and as seen from a comparison of the histograms of various distributions.

The performance of a model-based watermark detector or decoder is highly influenced by the accuracy of the model itself. There have been only a few watermarking detectors and decoders using HMM in the literature. The purpose of a watermark detector is only to determine whether a specific watermark is present or not in the received signal, whereas in a watermark decoder, the embedded watermark is considered as a hidden message that needs to be extracted accurately. An adaptive watermark detector has been proposed in [21] using HMM and the receiver operating characteristic (ROC) has been derived. However, the simulation results on the derived ROC have not been reported. A locally optimum additive watermark detector using vector-based HMM has been proposed in [11] and [12]. Theoretical expression for ROC has been derived, and the detector performance evaluated in terms of ROC against various kinds of attacks. An additive watermark decoder based on HMM using a convolution code has been proposed in [22]. However, the performance has been evaluated only in the presence of the JPEG compression. An informed additive decoder using HMM in the wavelet domain has been proposed in [23]. The robustness of the method against various attacks, such as JPEG compression and additive noise, has been studied. However, the HMM parameters need to be sent as a side information to the receiver. An informed watermarking scheme using posterior HMM has been proposed in [24] in which the HMM parameters are transmitted to the receiver, and reestimated. In an effort to develop a blind watermarking scheme without the need for transmitting any additional information to the receiver, in this paper, we propose an optimum multiplicative watermark decoder in the wavelet domain using the vector-based HMM distribution. The purpose of this paper is to extract the watermark message using only the watermarked image as received. The proposed decoder can be expected to offer a better performance and provide a higher robustness against various kinds of attacks compared with that of the other existing methods, in view of the fact that the vector-based HMM distribution provides a close fit as mentioned previously, and that multiplicative watermarking approach is content-dependent. The decoder is designed using the maximum likelihood method. Closed-form expression for the bit error rate (BER) of the proposed decoder is derived and validated experimentally. The performance of the proposed decoder is investigated through several experiments and compared with those of the other existing decoders. The robustness of the proposed scheme is examined when the watermarked images are subjected to various kinds of attacks, such as JPEG compression, Gaussian noise, salt and pepper noise, median filtering, rotation, and gamma correction, and compared with that of the other decoders.

This paper is organized as follows. In Section II, the embedding part of the proposed multiplicative watermarking technique is explained. In Section III, an optimum watermark decoder using the vector-based HMM is proposed, and theoretical performance analysis is presented. Section IV provides simulation results, and Section V concludes this paper.

II. WATERMARK EMBEDDING

Digital image watermarking technique consists of two parts, namely, embedding and decoding/detection. In the former part, the watermark signal is inserted into the host image, whereas in the decoding part the watermark bits are extracted. In this paper, the embedding is carried out in the following manner.

The host image I, a grayscale image of size $N_I \times N_I$, is first decomposed by a two-level wavelet transform. In order to embed the watermark bits, the variance of each subband in the second level is calculated, and the subband with the maximum variance is selected for inserting the watermark. Let $\mathbf{x} = \{x_1, x_2, \ldots, x_N\}$ be the set of the magnitudes of the wavelet coefficients of the selected subband. The set $\mathbf{x}$ is divided into N_b nonoverlapping equal-sized blocks $B_1, B_2, \ldots, B_{N_b}$, and let $\mathbf{m} = \{m_1, m_2, \ldots, m_N\}$ be a pseudorandom sequence, where m_i takes the value -1 or 1 with equal probability. The watermark bits w are generated using $w_i = m_1 b_k$ and $i = 1, \ldots, N, k = \lceil((iN_b)/N)\rceil$, where $\mathbf{b} = \{b_1, b_2, \ldots, b_N\}$ are message bits that can have values -1 and 1. It should be noted that the same bit b_k is used for all the coefficients in the block B_k to obtain the watermark bits. The set of watermarked coefficients $\mathbf{y} = \{y_1, y_2, \ldots, y_N\}$ is obtained as

$$y_i = (1 + \alpha w_i)x_i \tag{1}$$

where α is a positive weighting factor that provides a tradeoff between the robustness of the watermarking scheme and the imperceptibility of the embedded watermark. The weighting factor α is obtained by taking into account the human visual system properties. This can be realized by using the watermark-to-document ratio (WDR), given in [6], $\text{WDR} = 20 \log_{10}((\sum_i \alpha w_i)/(\sum_i x_i))$, where the numerator is the energy of the weighted watermark bits, and the denominator is the energy of the host-selected subband wavelet coefficients. The watermarked image is then obtained by applying the inverse wavelet transform to the marked coefficients. The block diagram for the proposed embedding scheme is shown in Fig. 1.

III. WATERMARK DECODER

The blind watermark decoder to be designed in this section is based on the statistical properties of the wavelet coefficients of the image. The wavelet coefficients are modeled using the vector-based HMM, which is superior to other models in characterizing the statistical properties of the wavelet coefficients and in taking into account their dependencies across scales and orientations. Since the performance of a decoder is highly dependent on the accuracy of the model, we can expect the proposed decoder to provide a performance better than that of the other decoders using wavelets.

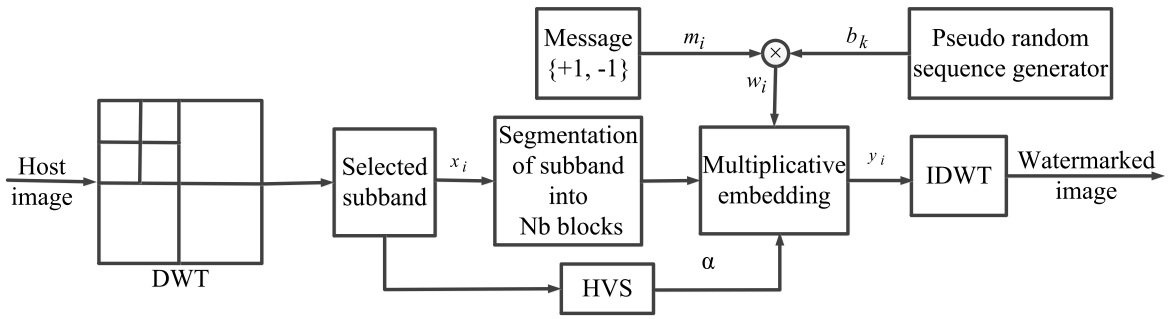

Fig. 1. Proposed watermark embedding scheme in the wavelet domain.

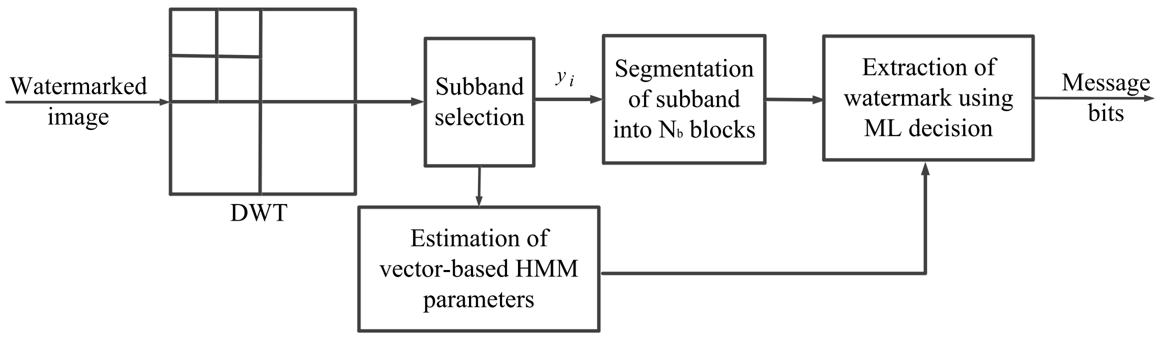

Fig. 2. Proposed watermark decoding scheme using the vector-based HMM in the wavelet domain.

A. Modeling the Wavelet Coefficients Using the Vector-Based HMM

In an M-state vector-based HMM, for each wavelet coefficient in ith node and the jth scale x_{ij}, there is a hidden state S_{ij} with a probability mass function $p(S_{ij} = m) = p_j^m, m = 1, 2, \ldots, M$. Conditioning on $S_{ij} = m$, vector $\mathbf{x}_{ij}$ of the wavelet coefficients follows a multivariate Gaussian function with mean μ_j^m and covariance matrix C_j^m. If x_{ij}^d denotes the wavelet coefficients at orientation d: HL, LH, or HH, the grouping process yields the vectors of coefficients as $x_{ij} = [x_{ij}^{HL}, x_{ij}^{LH}, x_{ij}^{HH}]^T$. The cross correlation of these three wavelet coefficients can be described by their covariance matrix C_j^m. The marginal distribution of the wavelet coefficient in ith node and the jth scale can be expressed as [12]

$$f_X(\mathbf{x}_{ij}) = \sum_{m=1}^{M} \frac{p_j^m \exp\left\{-\frac{1}{2}\left(\mathbf{x}_{ij} - \mu_j^m\right)^T \left(C_j^m\right)^{-1}\left(\mathbf{x}_{ij} - \mu_j^m\right)\right\}}{\sqrt{(2\pi)^3\left|\det\left(C_j^m\right)\right|}}. \tag{2}$$

In the vector-based HMM, the wavelet coefficients at the same scale and location, but in different orientations, are tied so as to have the same hidden states.

B. Proposed Optimum Watermark Decoder

In a multibit watermarking scheme, the role of a decoder is to extract the hidden binary message sequence from the watermarked image. The scheme for the proposed watermark decoder is shown in Fig. 2. The watermarked image is decomposed by a two-level wavelet transform, and the coefficients y of the selected subband (the one with the maximum variance) are divided into N_b nonoverlapping equal-sized blocks. A binary bit message b_k of -1 or 1 is embedded in the kth block as

$$\begin{aligned} H_1 &: y_i = (1 + \alpha m_i)x_i, \quad b_k = 1 \\ H_0 &: y_i = (1 - \alpha m_i)x_i, \quad b_k = -1 \end{aligned} \tag{3}$$

where $i \in B_k$, the kth block and x_i's and y_i's are the corresponding host and watermarked coefficients. It should be noted that the bits of the binary message sequence are assumed to be equally probable. In order to extract the hidden message bit in the block B_k of the wavelet coefficients of the selected subband of the watermarked image, an optimum decoder based on the maximum likelihood decision is developed and formulated as

$$\prod_{i \in B_k} f_Y(y_i|b_k = 1) \underset{H_0}{\overset{H_1}{\gtrless}} \prod_{i \in B_k} f_Y(y_i|b_k = -1). \tag{4}$$

Applying the natural logarithm on both the sides of this equation, the optimum decoder $l_k(y)$ can be obtained as

$$l_k(y) = \sum_{i \in B_k} \ln \frac{f_Y(y_i|b_k = 1)}{f_Y(y_i|b_k = -1)} \underset{H_0}{\overset{H_1}{\gtrless}} 0. \tag{5}$$

In order to calculate $l_k(y)$, we note that the statistical models for $f_Y(y_i|b_k = \pm 1)$ are $f_Y(y_i|b_k = \pm 1) = (1/(1 \pm \alpha m_i)) f_X((y_i)/(1 \pm \alpha m_i))$, where $f_X(x)$ indicates the pdf of the wavelet coefficients of the selected subband of the host image. To obtain the pdf, $f_X((y_i)/(1 \pm \alpha m_i))$, we make use of the M-state vector-based HMM marginal distribution given in (2). Since the watermarking is performed at the second level of the wavelet transform, j in (2) assumes the value $(\log_2 N_I)-2$, which for simplicity is denoted by q. Thus, $l_k(y)$ can be obtained after some algebraic manipulations as

$$l_k(y) = \sum_{i\in B_k} \ln \frac{1-\alpha m_i}{1+\alpha m_i} + \sum_{i\in B_k} \ln \frac{\sum_{m=1}^{M} \frac{p_q^m \exp\left\{\frac{-1}{2}\left(\frac{\mathbf{y}_i}{1+\alpha m_i}-\mu_q^m\right)^T \left(C_q^m\right)^{-1}\left(\frac{\mathbf{y}_i}{1+\alpha m_i}-\mu_q^m\right)\right\}}{\sqrt{\left|\det\left(C_q^m\right)\right|}}}{\sum_{m=1}^{M} \frac{p_q^m \exp\left\{\frac{-1}{2}\left(\frac{\mathbf{y}_i}{1-\alpha m_i}-\mu_q^m\right)^T \left(C_q^m\right)^{-1}\left(\frac{\mathbf{y}_i}{1-\alpha m_i}-\mu_q^m\right)\right\}}{\sqrt{\left|\det\left(C_q^m\right)\right|}}}. \tag{6}$$

The kth message bit present in the coefficients can be decoded as

$$\hat{b}_k = \begin{cases} 1, & Z_k(y) > T_k \\ -1, & Z_k(y) < T_k \end{cases} \tag{7}$$

where

$$Z_k = \sum_{i\in B_k} \ln \frac{\sum_{m=1}^{M} \frac{p_q^m \exp\left\{\frac{-1}{2}\left(\frac{\mathbf{y}_i}{1+\alpha m_i}-\mu_q^m\right)^T \left(C_q^m\right)^{-1}\left(\frac{\mathbf{y}_i}{1+\alpha m_i}-\mu_q^m\right)\right\}}{\sqrt{\left|\det\left(C_q^m\right)\right|}}}{\sum_{m=1}^{M} \frac{p_q^m \exp\left\{\frac{-1}{2}\left(\frac{\mathbf{y}_i}{1-\alpha m_i}-\mu_q^m\right)^T \left(C_q^m\right)^{-1}\left(\frac{\mathbf{y}_i}{1-\alpha m_i}-\mu_q^m\right)\right\}}{\sqrt{\left|\det\left(C_q^m\right)\right|}}}$$

$$T_k = \sum_{i\in B_k} \ln \frac{1-\alpha m_i}{1+\alpha m_i}. \tag{8}$$

C. Error Analysis

The bit error probability, also called BER, is used to analyze the performance of the proposed watermark decoder. The bit error probability is computed in the absence of any attack. For the optimum decoder, the bit error probability is given by

$$P_e = \frac{1}{N_B} \sum_{k=1}^{N_B} [P(Z_k(y) > T_k|H_0) + P(Z_k(y) < T_k|H_1)]. \tag{9}$$

To find the probability under the condition of H_0, $y_i = (1-\alpha m_i)x_i$; hence $Z_k(y)$ is equal to

$$Z_k(y|H_0) = \sum_{i\in B_k} \ln \frac{\sum_{m=1}^{M} \frac{p_q^m \exp\left\{\frac{-1}{2}\left(\frac{1-\alpha m_i}{1+\alpha m_i}x_i-\mu_q^m\right)^T \left(C_q^m\right)^{-1}\left(\frac{1-\alpha m_i}{1+\alpha m_i}-\mu_q^m\right)\right\}}{\sqrt{\left|\det\left(C_q^m\right)\right|}}}{\sum_{m=1}^{M} \frac{p_q^m \exp\left\{\frac{-1}{2}\left(x_i-\mu_q^m\right)^T \left(C_q^m\right)^{-1}\left(x_i-\mu_q^m\right)\right\}}{\sqrt{\left|\det\left(C_q^m\right)\right|}}}. \tag{10}$$

Under the condition H_1, $y_i = (1+\alpha m_i)x_i$; therefore, $Z_k(y|H_0) = -Z_k(y|H_1)$. It is noted that the sequence m_i is an independent identical random process that can have two values -1 and 1 with equal probabilities. Since $Z_k(y|H_0)$ is the sum of a large number of independent random variables, according to the central limit theorem, it can be approximated by the Gaussian distribution with finite mean and variance under each hypothesis, i.e., (μ_0, σ_0^2) and (μ_1, σ_1^2) [5]. The mean under the hypothesis H_0, is given by (11), as shown at the bottom of this page, which can be simplified to

$$\mu_0 = \sum_{i\in B_k} \ln \frac{\sqrt{a_i b_i}}{c_i} \tag{12}$$

where

$$a_i = \sum_{m=1}^{M} \frac{p_q^m \exp\left\{\frac{-1}{2}\left(\frac{1-\alpha m_i}{1+\alpha m_i}x_i-\mu_q^m\right)^T \left(C_q^m\right)^{-1}\left(\frac{1-\alpha m_i}{1+\alpha m_i}x_i-\mu_q^m\right)\right\}}{\sqrt{\left|\det\left(C_q^m\right)\right|}}$$

$$b_i = \sum_{m=1}^{M} \frac{p_q^m \exp\left\{\frac{-1}{2}\left(\frac{1+\alpha m_i}{1-\alpha m_i}x_i-\mu_q^m\right)^T \left(C_q^m\right)^{-1}\left(\frac{1+\alpha m_i}{1-\alpha m_i}x_i-\mu_q^m\right)\right\}}{\sqrt{\left|\det\left(C_q^m\right)\right|}}$$

$$c_i = \sum_{m=1}^{M} \frac{p_q^m \exp\left\{\frac{-1}{2}\left(x_i-\mu_q^m\right)^T \left(C_q^m\right)^{-1}\left(x_i-\mu_q^m\right)\right\}}{\sqrt{\left|\det\left(C_q^m\right)\right|}}. \tag{13}$$

The variance σ_0^2 is given by

$$\begin{aligned}\sigma_0^2 &= E[Z_k(y|H_0) - \mu_0^2] \\ &= \frac{1}{4}\sum_{i\in B_k}\left(\ln\frac{a_i}{b_i}\right)^2.\end{aligned} \tag{14}$$

$$\begin{aligned}\mu_0 &= E[Z_k(y|H_0)] \\ &= \sum_{i\in B_k}\Bigg(\frac{1}{2}\ln\sum_{m=1}^{M} \frac{p_q^m \exp\left\{\frac{-1}{2}\left(\frac{1-\alpha m_i}{1+\alpha m_i}x_i-\mu_q^m\right)^T \left(C_q^m\right)^{-1}\left(\frac{1-\alpha m_i}{1+\alpha m_i}x_i-\mu_q^m\right)\right\}}{\sqrt{\left|\det\left(C_q^m\right)\right|}} \\ &\quad +\frac{1}{2}\ln\sum_{m=1}^{M} \frac{p_q^m \exp\left\{\frac{-1}{2}\left(\frac{1+\alpha m_i}{1-\alpha m_i}x_i-\mu_q^m\right)^T \left(C_q^m\right)^{-1}\left(\frac{1+\alpha m_i}{1-\alpha m_i}x_i-\mu_q^m\right)\right\}}{\sqrt{\left|\det\left(C_q^m\right)\right|}} \\ &\quad -\ln\sum_{m=1}^{M} \frac{p_q^m \exp\left\{\frac{-1}{2}\left(x_i-\mu_q^m\right)^T \left(C_q^m\right)^{-1}\left(x_i-\mu_q^m\right)\right\}}{\sqrt{\left|\det\left(C_q^m\right)\right|}}\Bigg)\end{aligned} \tag{11}$$

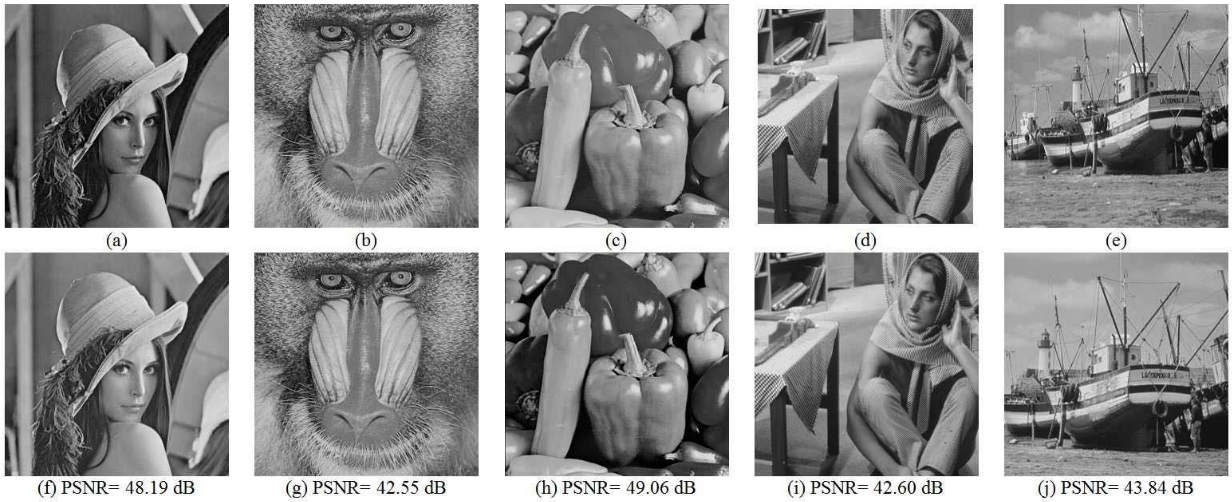

Fig. 3. (a)–(e) Original and (f)–(j) watermarked images for WDR = −42 dB.

Since $Z_k(y|H_0) = -Z_k(y|H_1)$, we have $\mu_1 = -\mu_0$ and $\sigma_1 = \sigma_0$. The error probability P_e^k for decoding a watermark bit is obtained as

$$\begin{aligned} P_e^k &= \frac{1}{2}\{P(Z_k(y) > T_k|H_0) + P(Z_k(y) < T_k|H_1)\} \\ &= \frac{1}{2}\left[1 + Q\left(\frac{T_k - \mu_0}{\sigma_0}\right) - Q\left(\frac{T_k - \mu_1}{\sigma_1}\right)\right] \\ &= \frac{1}{2}\left[1 + Q\left(\frac{T_k - \mu_0}{\sigma_0}\right) - Q\left(\frac{T_k + \mu_0}{\sigma_0}\right)\right] \end{aligned} \tag{15}$$

where $Q(x) = (1/(\sqrt{2\pi}))\int_x^\infty \exp((-t^2)/2)dt$. Thus, if the binary message bits −1 or 1 are embedded in the host image with the same probability, then the total BER is given by

$$P_e = \frac{1}{N_B}\sum_{k=1}^{N_B} P_e^k. \tag{16}$$

The performance of the proposed decoder is evaluated in terms of BER based on (16).

IV. Experimental Results

To evaluate the performance of the proposed vector-based HMM watermark decoder, extensive experiments are conducted on a large set of test images taken from [40]. In all the experiments, the 9/7 wavelet filter with two levels of decomposition is performed. The host and watermarked images corresponding to a few of the test images are shown in Fig. 3. The watermarks are embedded in the host images using the messages of length 128 bits with a WDR = −42 dB. It is seen from Fig. 3 that there is no noticeable difference between the original and the watermarked images, thus ensuring the imperceptibility of the embedded watermark. The objective measure of the peak signal-to-noise ratio (PSNR) between the original and watermarked images is used to evaluate this imperceptibility, and the values are also given in Fig. 3. The high PSNR values confirm the superior performance of the embedding scheme.

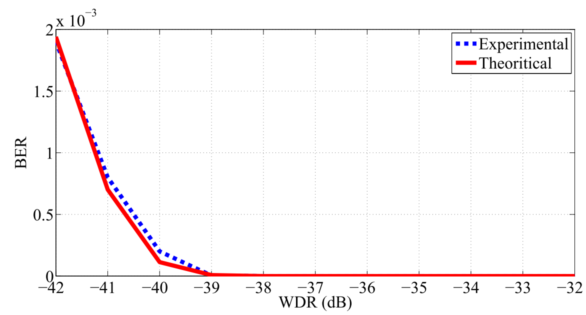

Fig. 4. Theoretical and experimental BER of the proposed decoder averaged over 96 test images with message length of 128 bits for different WDR values.

A. Performance of the Proposed Decoder Without Attack

In Section III, a theoretical expression for BER, as given by (16), was obtained; in order to calculate BER using (16), it is necessary to have the values of the parameters of the vector-based HMM for the wavelet coefficients of the original image. Since the watermark is embedded with a small value of α, these parameters of the vector-based HMM can be assumed to be the same for the original and watermarked images. Hence, these parameters are estimated from the watermarked coefficient y.

In order to validate the theoretical values of BER obtained from (16), comparisons are now made with the experimental BER obtained from Monte Carlo simulations. To this end, for each of the 96 test images, 1000 pseudorandom message sequences are generated, and each sequence embedded in the test image for a given WDR, and decoded using (7). The number of errors is computed for each run, and the experimental BER averaged over the 1000 runs. Fig. 4 shows the theoretical and experimental BER values of the proposed decoder averaged over the test images for various values of WDR. It is seen from Fig. 4 that the BER values obtained theoretically are very close to the experimental ones, thus validating the expression for BER given by (16).

The performance of the proposed watermark decoder in the wavelet domain by using the vector-based HMM is examined

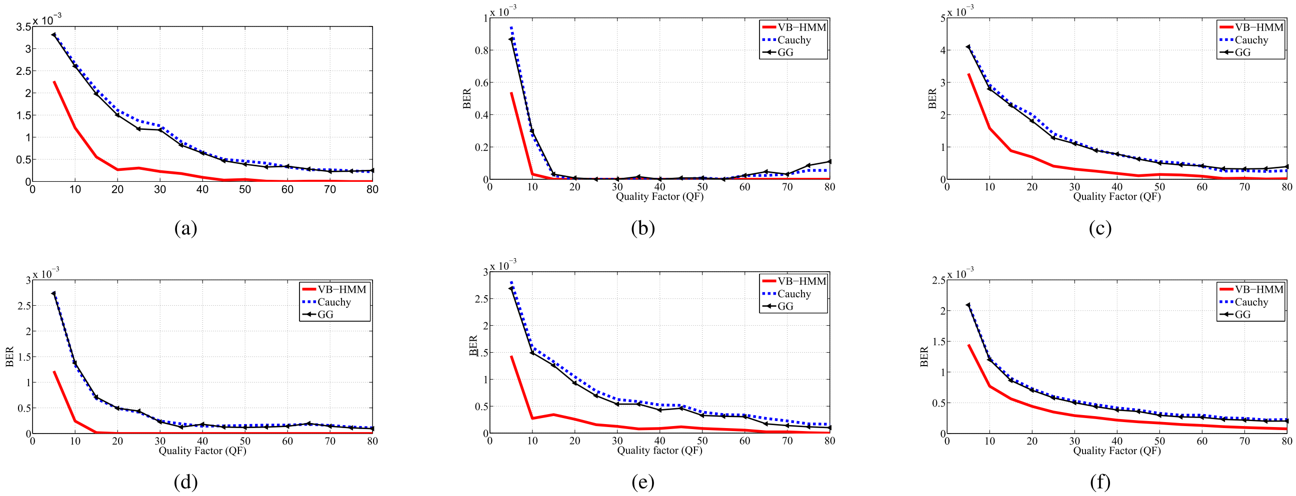

Fig. 5. BER values of the extracted watermark obtained using the proposed VB-HMM, GG, and Cauchy decoders when images are JPEG-compressed with different quality factors. (a) *Lena*. (b) *Baboon*. (c) *Peppers*. (d) *Barbara*. (e) *Boat*. (f) Averaged over 96 different images.

TABLE I

BER VALUES OBTAINED USING VARIOUS DECODERS FOR DIFFERENT IMAGES WHEN MESSAGE LENGTH IS 64 AND 128 BITS, AND WDR = −42 dB

Image	VB-HMM	Cauchy	GG
	Message length = 64 bits		
Lena	**0.001281**	0.001781	0.002375
Baboon	**0.001141**	0.001445	0.001563
Peppers	**0.001391**	0.001578	0.001938
Barbara	**0.000406**	0.001148	0.001875
Boat	**0.000563**	0.001563	0.002094
Airplane	**0.000664**	0.001164	0.002023
Man	**0.000578**	0.000820	0.001609
Zelda	**0.001707**	0.001977	0.002477
Elaine	**0.001195**	0.001680	0.001961
Lake	**0.001077**	0.001531	0.001820
Average	**0.001000**	0.001468	0.001973
	Message length = 128 bits		
Lena	**0.002273**	0.003609	0.004164
Baboon	**0.001117**	0.001852	0.002906
Peppers	**0.002406**	0.002898	0.003945
Barbara	**0.000906**	0.003234	0.004305
Boat	**0.001891**	0.003383	0.004188
Airplane	**0.002039**	0.003047	0.004188
Man	**0.001109**	0.002516	0.003578
Zelda	**0.002891**	0.004063	0.003516
Elaine	**0.002992**	0.003875	0.004328
Lake	**0.001758**	0.002922	0.003922
Average	**0.001938**	0.003139	0.003485

TABLE II

BER VALUES OF THE EXTRACTED WATERMARK OBTAINED USING THE PROPOSED VB-HMM, GG, AND CAUCHY DECODERS WHEN IMAGES ARE CORRUPTED BY SALT AND PEPPER NOISE $p = 0.05$ AND $p = 0.1$

Image	VB-HMM	Cauchy	GG
		p = 0.05	
Lena	**0.0011**	0.0430	0.0203
Baboon	**0**	**0**	**0**
peppers	**0.0007**	0.0313	0.0133
Barbara	**0**	0.0016	0.0007
Boat	**0.0013**	0.0375	0.0219
Airplane	**0.0023**	0.0453	0.0156
Man	**0**	0.0086	0.0016
Zelda	**0.0070**	0.1086	0.0508
Elaine	**0.0082**	0.1391	0.0563
Lake	**0**	0.0375	0.0094
Average	**0.0020**	0.0452	0.0189
		p = 0.1	
Lena	**0.0076**	0.1156	0.0867
Baboon	**0**	**0**	**0**
peppers	**0.0078**	0.1211	0.0961
Barbara	**0.0015**	0.0227	0.0109
Boat	**0.0044**	0.0820	0.0531
Airplane	**0.0069**	0.1109	0.0875
Man	**0.0013**	0.0109	0.0094
Zelda	**0.0165**	0.1852	0.2102
Elaine	**0.0214**	0.2156	0.2016
Lake	**0.0009**	0.0597	0.0133
Average	**0.0068**	0.0923	0.0767

and compared with that yielded by using the Cauchy [6] and GG [5], [19] decoders. For this purpose, we use the same framework as shown in Fig. 2 for all the decoders employing the proposed vector-based HMM, Cauchy, or GG distributions for the wavelet coefficients. Table I gives the BER values obtained using the proposed decoder as well as that obtained using the Cauchy and GG-based decoders with message lengths of 64 and 128 bits and WDR = −42 dB for a number of test images, namley, *Lena*, *Baboon*, *Peppers*, *Barbara*, *Boat*, *Airplane*, *Man*, *Zelda*, *Elaine*, and *Lake*, and the average over all these images. It is seen from Table I that the proposed vector-based HMM decoder provides a BER that is lower than that provided by the other decoders.

B. Performance of the Proposed Decoder Against Attacks

The robustness of the proposed decoder is now studied against common attacks, such as JPEG compression, Gaussian noise, salt and pepper noise, median filtering, rotation, and Gamma correction. The results reported in Section IV.B are for a message length of 128 bits and a WDR = −38 dB.

1) JPEG Compression: Studying the robustness of a watermark decoder against JPEG compression attack is very important in view of its popularity in Internet applications. The results of BER when the test images, *Lena*, *Baboon*, *Peppers*, *Barbara*, and *Boat*, are JPEG-compressed with quality factor changing from 5 to 80 are shown in Fig. 5(a)–(e). The BER values averaged over 96 different test images are shown

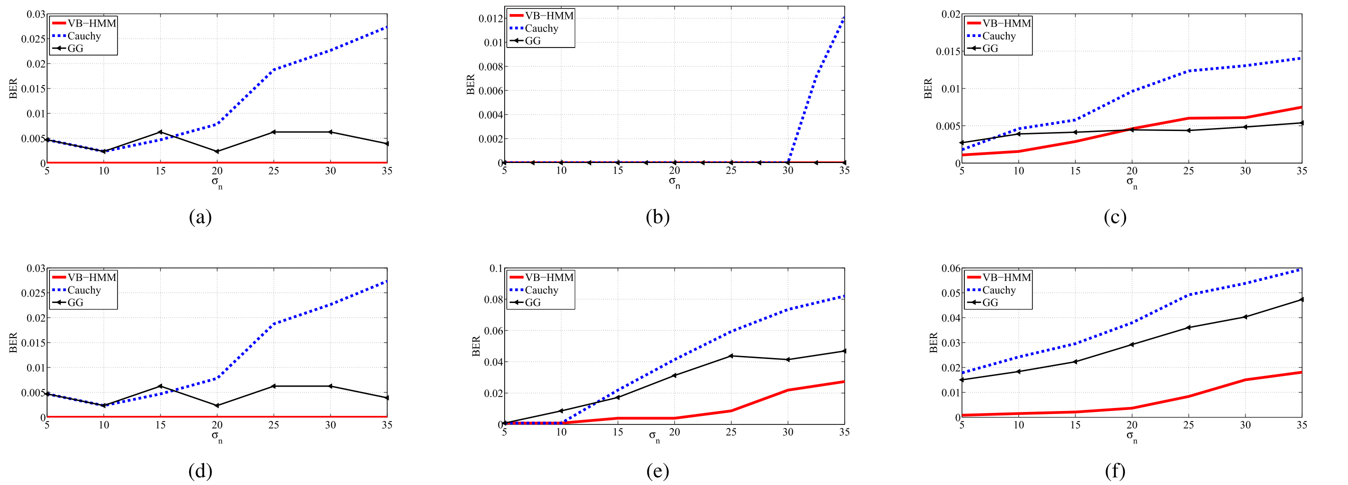

Fig. 6. BER values of the extracted watermark obtained using the proposed VB-HMM, GG, and Cauchy decoders when images are corrupted by additive Gaussian noise with different σ_n values. (a) *Lena*. (b) *Baboon*. (c) *Peppers*. (d) *Barbara*. (e) *Boat*. (f) Averaged over 96 different images.

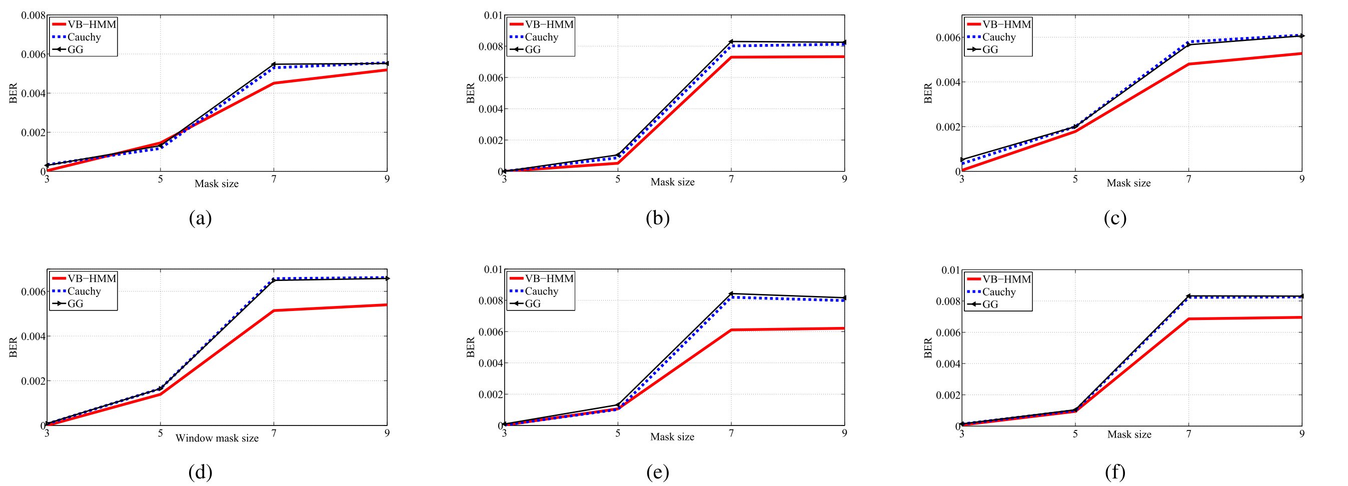

Fig. 7. BER values of the extracted watermark obtained using the proposed VB-HMM, GG, and Cauchy decoders when images undergo median filtering with different window sizes. (a) *Lena*. (b) *Baboon*. (c) *Peppers*. (d) *Barbara*. (e) *Boat*. (f) Averaged over 96 different images.

in Fig. 5(f). It can be seen from Fig. 5 that the proposed decoder is more robust against JPEG compression in comparison with the GG and Cauchy decoders. It is to be noted that for practical compression range of still images, i.e., QF > 50, the BER value approaches zero for the proposed decoder.

2) Additive Gaussian Noise: The results of BER when the test images, *Lena*, *Baboon*, *Peppers*, *Barbara*, and *Boat*, are contaminated by the additive Gaussian noise with noise standard deviation σ_n varying from 5 to 35 are shown in Fig. 6(a)–(e). The BER values averaged over 96 different test images when the images are contaminated by different levels of additive Gaussian noise are shown in Fig. 6(f). It can be seen from Fig. 6 that the proposed watermarking scheme using the vector-based HMM exhibits a better performance in the presence of Gaussian noise compared with that provided by the decoders based on the GG and Cauchy distributions, especially for higher noise levels, except for the case of the image *Peppers*.

3) Salt and Pepper Noise: Salt and pepper noise is the most commonly long-tailed noise used in image processing. The results of the BER, when the different test images corrupted by the salt and pepper noise, are shown in Table II. It can be seen from Table II that the proposed watermarking scheme is more robust against salt and pepper noise in comparison with that yielded by the GG and Cauchy-based decoders. It can also be seen from Table I that the decoders can perfectly extract the watermark bits in the case of the *Baboon* image.

4) Median Filtering: Robustness of watermark decoder against median filtering, a nonlinear filter, is a challenging task, since it might destroy the watermark severely. The results of BER when the test images, *Lena*, *Baboon*, *Peppers*, *Barbara*, and *Boat*, undergo median filtering with window sizes 3×3, 5×5, 7×7, and 9×9 are shown in Fig. 7(a)–(e), respectively. The BER values averaged over 96 test images when the images are median-filtered are shown in Fig. 7(f). It can be seen from Fig. 7 that the proposed scheme is more robust against median filtering in comparison with the GG and Cauchy-based schemes especially when the window size is bigger than 3×3.

5) Gamma Correction: The performance of the proposed decoder is then investigated and compared with the Cauchy and GG-based decoders against the gamma correction attack.

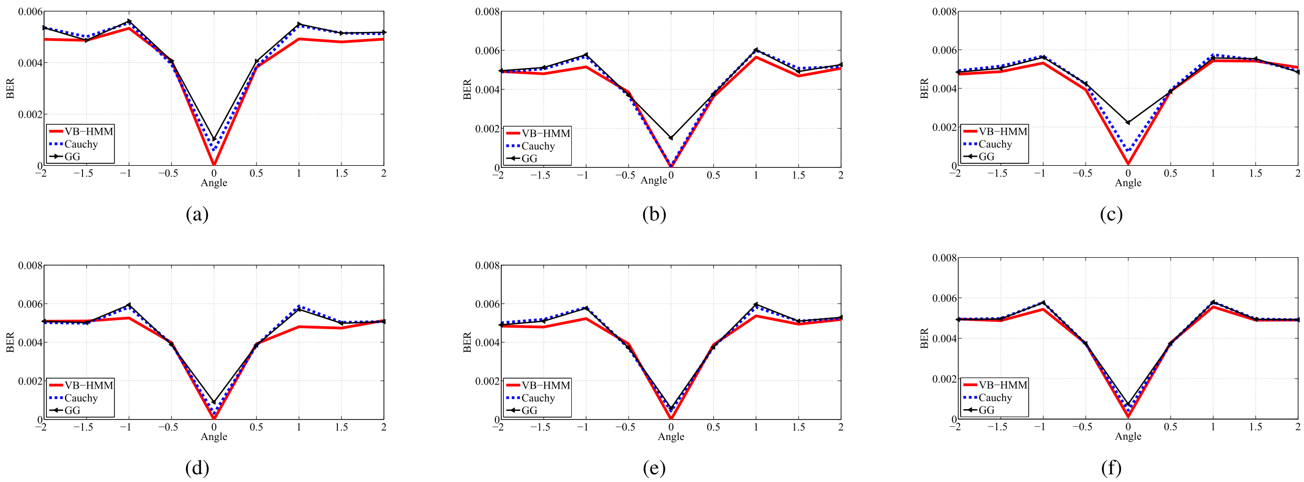

Fig. 8. BER values of the extracted watermark obtained using the proposed VB-HMM, GG, and Cauchy decoders when images are rotated by different angles. (a) *Lena*. (b) *Baboon*. (c) *Peppers*. (d) *Barbara*. (e) *Boat*. (f) Averaged over 96 different images.

TABLE III

BER VALUES OF THE EXTRACTED WATERMARK OBTAINED USING THE PROPOSED VB-HMM, GG, AND CAUCHY DECODERS WHEN IMAGES UNDERGO GAMMA CORRECTION WITH DIFFERENT VALUES OF GAMMA

γ	2	1.5	0.9	0.75
	Lena			
VB-HMM	**0.1030**	**0.1164**	**0.1194**	**0.1144**
Cauchy	0.1189	0.2867	0.2891	0.2617
GG	0.3117	0.3133	0.3156	0.2961
	Baboon			
VB-HMM	**0.0345**	**0.0354**	**0.0358**	**0.0358**
Cauchy	0.2344	0.2250	0.2289	0.2266
GG	0.2641	0.2625	0.2500	0.2648
	Peppers			
VB-HMM	**0.1359**	**0.1409**	**0.1351**	**0.1385**
Cauchy	0.2695	0.2805	0.2555	0.2734
GG	0.2938	0.3016	0.2906	0.2984
	Barbara			
VB-HMM	**0**	**0**	**0**	**0**
Cauchy	0.0055	0.0547	0.1148	0.1414
GG	0.0055	0.0258	0.0437	0.0219
	Boat			
VB-HMM	**0**	**0.0023**	**0.0023**	**0.0023**
Cauchy	0.0219	0.1133	0.1220	0.1422
GG	0.0187	0.0367	0.0773	0.0641

Table III gives the BERs when the test images undergo gamma correction with different gamma values 2, 1.5, 0.9, and 0.75. It is seen from Table III that the proposed vector-based HMM decoder is more robust against Gamma correction compared with the Cauchy and GG-based decoders.

6) Rotation: We then investigate the robustness of the proposed watermarking scheme using the vector-based HMM decoder against rotation attack and compare it with schemes using GG and Cauchy-based decoders. The results of BER when the test images, *Lena*, *Baboon*, *Peppers*, *Barbara*, and *Boat*, are rotated with different angles are shown in Fig. 8(a)–(e), respectively. The BER values averaged over 96 different test images when the images are rotated by various angles are shown in Fig. 8(f). It can be seen from Fig. 8 that the proposed method is more robust against rotation as compared with the GG and Cauchy-based schemes.

TABLE IV

BERS OBTAINED USING THE PROPOSED WATERMARKING SCHEME AS WELL AS THOSE OBTAINED USING THE SCHEMES IN [13], [17], AND [15] WHEN WATERMARKED IMAGES ARE UNDER VARIOUS ATTACKS (MESSAGE LENGTH = 256 BITS AND PSNR = 42 dB)

	VB-HMM	[13]	[17]	[15]
	Barbara			
JPEG (QF = 11)	**0**	0.1645	0.0043	0.0964
AWGN ($\sigma_n = 10$)	**0**	0.0145	**0**	0.0140
Median filter (3×3)	**0**	0.2495	0.0503	0.0110
	Baboon			
JPEG (QF = 11)	**0.0015**	0.1695	0.0073	0.0986
AWGN ($\sigma_n = 10$)	**0**	0.0130	**0**	0.0128
Median filter (3×3)	**0**	0.3165	0.0160	0.0503
	Peppers			
JPEG (QF = 11)	**0.0033**	0.2610	0.0055	0.1068
AWGN ($\sigma_n = 10$)	**0**	0.0125	0.0007	0.0132
Median filter (3×3)	**0**	0.2935	0.0016	0.0117
	Lena			
JPEG (QF = 11)	**0.028**	0.2980	NA	0.0864
AWGN ($\sigma_n = 10$)	**0**	0.0145	NA	0.0185
Median filter (3×3)	**0**	0.3080	NA	**0**

TABLE V

BER VALUES OBTAINED USING THE PROPOSED VB-HMM-BASED WATERMARKING SCHEME AS WELL AS THAT OBTAINED USING THE SCHEMES IN [15] AND [28] WHEN WATERMARKED IMAGES ARE UNDER VARIOUS ATTACKS (MESSAGE LENGTH = 128 BITS)

	VB-HMM	[28]	[15]
	Barbara, PSNR = 36 dB		
JPEG (QF = 20)	**0**	0.004	**0**
AWGN ($\sigma_n = 20$)	**0.003**	**0.001**	0.0107
salt & pepper ($p = 0.05$)	**0**	0.0148	0.0043
	Baboon, PSNR = 39 dB		
JPEG (QF = 20)	**0**	0.0189	**0**
AWGN ($\sigma_n = 20$)	**0.0013**	0.0030	0.0148
salt & pepper ($p = 0.05$)	**0**	0.0289	0.0089

C. Comparison With Other Watermarking Methods

In order to further investigate the performance of the proposed method, we now compare the performance of the proposed vector-based HMM decoder with that of the

TABLE VI

BER VALUES OBTAINED USING THE PROPOSED WATERMARKING SCHEME AS WELL AS THAT OBTAINED USING THE SCHEMES IN [15], [17], [20], AND [26] WHEN WATERMARKED IMAGES ARE UNDER VARIOUS ATTACKS (MESSAGE LENGTH = 64 BITS AND PSNR = 42 dB)

	VB-HMM	[17]	[15]	[20]	[26]
			Peppers		
JPEG (QF = 5)	**0.0032**	0.0078	NA	0.0625	NA
JPEG (QF = 20)	**0**	**0**	0.0006	**0**	NA
Median filter (5 × 5)	0.0015	**0**	0.0156	0.0781	0.0531
Median filter (7 × 7)	0.0004	**0**	**0**	0.0936	0.1718
Median filter (9 × 9)	**0.0005**	0.0300	0.0462	0.5156	0.2875
Salt & pepper ($p = 0.08$)	**0.0003**	NA	0.0040	0.0251	NA
Rotation ($\theta = 0.5°$)	**0.0041**	0	0.2287	0.4063	NA
			Baboon		
JPEG (QF = 5)	0.0005	**0**	NA	0.0469	NA
JPEG (QF = 20)	**0**	**0**	**0**	**0**	NA
Median filter (5 × 5)	**0.0013**	0.0155	0.0050	0.1250	0.2093
Median filter (7 × 7)	**0.0042**	0.0488	0.0381	0.1250	0.3062
Median filter (9 × 9)	**0.0049**	0.0088	0.1231	0.7813	0.3500
Salt & pepper ($p = 0.08$)	**0**	NA	0.004	0.0334	NA
Rotation ($\theta = 0.5°$)	**0.0053**	0.0333	0.2081	0.4531	NA
			Lena		
JPEG (QF = 5)	**0.0002**	NA	NA	NA	NA
JPEG (QF = 20)	**0**	NA	**0**	**0**	NA
Median filter (5 × 5)	**0**	NA	**0**	0.0938	NA
Median filter (7 × 7)	**0**	NA	0.0065	0.1250	NA
Median filter (9 × 9)	**0.035**	NA	0.0384	0.5156	NA
Salt & pepper ($p = 0.08$)	**0.0013**	NA	0.0028	0.0267	NA
Rotation ($\theta = 0.5°$)	**0.0044**	NA	0.2087	0.4375	0.0546

state-of-the-art methods [13], [15]–[17], [20], [22]–[24], [26], [28]. In order to make a fair comparison, for a given message length, we set the PSNR values of the watermarked images in our proposed method to be the same as the values reported in these other works. Table IV gives the BER values of the proposed decoder and those given in [13], [17], and [15], for an embedded message of 256 bits against different attacks, namely, JPEG compression with QF $= 11$, additive Gaussian noise with $\sigma_n = 10$, and median filtering with a window of size 3×3 for the test images, *Barbara*, *Baboon*, *Peppers*, and *Lena*. It is seen from Table IV that the proposed watermark decoder is more robust than the others against these attacks.

In Table V, we compare the robustness of the proposed decoder for an embedded message of 128 bits with that of the works in [15] and [28], when the watermarked *Barbara* and *Baboon* images undergo JPEG compression with QF $= 20$, additive noise with $\sigma_n = 20$, and salt and pepper noise with $p = 0.05$. It is seen from Table V that the proposed decoder provides lower BERs than that provided by the other decoders, indicating its higher robustness.

Table VI gives the BER values for the proposed decoder and those in [15], [17], [20], and [26] for an embedded message of 64 bits against different attacks, namely, JPEG compression with QF $= 5$ and 20, median filtering with window size 5×5, 7×7, and 9×9, salt and pepper noise with $p = 0.08$, and rotation of 0.5°, for the test images, *Peppers*, *Baboon*, and *Lena*. It is seen from Table VI that the proposed watermark decoder is more robust than the other decoders against these attacks.

Table VII gives the BER values for the proposed decoder for an embedded message of 128 bits as well as that of the methods in [15] and [16], when the *Lena* image is contaminated by the additive Gaussian noise for various values of the noise standard deviation and is JPEG-compressed with different values of quality factor. It is seen from Table VII that the proposed vector-based HMM decoder outperforms those in [15] and [16] by providing the lowest BER values.

TABLE VII

BER VALUES OF THE EXTRACTED WATERMARK OBTAINED USING THE PROPOSED VB-HMM-BASED WATERMARKING SCHEME AS WELL AS THAT OBTAINED USING THE SCHEMES IN [15] AND [16], WHEN WATERMARKED *Lena* IMAGE IS UNDER VARIOUS ATTACKS (MESSAGE LENGTH = 128 BITS AND PSNR = 45 dB)

	VB-HMM	[16]	[15]
σ_n		AWGN	
5	**0**	**0**	**0**
20	**0.0215**	0.1016	0.0234
35	**0.0817**	0.1344	0.2031
QF		JPEG	
4	**0.0021**	0.375	0.3203
10	**0.0012**	0.0391	0.0625
16	**0**	**0**	**0**
20	**0**	**0**	**0**

In order to compare the performance of the proposed decoder with that of [22], we insert a 60-bits message into different test images of size 512×512. The results in terms of PSNR of the watermarked image and the BER in the presence of JPEG compression are shown in Tables VIII and IX, respectively. It is seen from Tables VIII and IX that the proposed method has better imperceptibility in comparison with that of [22] by providing higher PSNR values, and it is more robust against JPEG compression by providing lower BER values.

It should be noted that the PSNR value of the watermarked *Lena* image of size 256×256 pixels and a message of

TABLE VIII
PSNR VALUES OBTAINED USING THE PROPOSED METHOD AND THE METHOD IN [22]

Image	Proposed	[22]
Lena	**49.13**	42.56
Baboon	**47.23**	42.98
Peppers	**49.99**	42.23
Boat	**47.56**	42.43

TABLE IX
BER VALUES OBTAINED USING DIFFERENT DECODERS WHEN THE IMAGES ARE JPEG-COMPRESSED WITH DIFFERENT VALUES OF QF

QF	15	20	25	30	35	40
	Lena					
Proposed	**0**	**0**	**0**	**0**	**0**	**0**
[22]	0.159	0.102	0.22	0.028	0.018	0.017
	Baboon					
Proposed	**0**	**0**	**0**	**0**	**0**	**0**
[22]	0.142	0.134	0.09	0.081	0.075	0.071
	Peppers					
Proposed	**0.0002**	**0**	**0**	**0**	**0**	**0**
[22]	0.11	0.39	0.021	0.017	0.008	0.004
	Boat					
Proposed	**0**	**0**	**0**	**0**	**0**	**0**
[22]	0.128	0.078	0.07	0.038	0.018	0.018

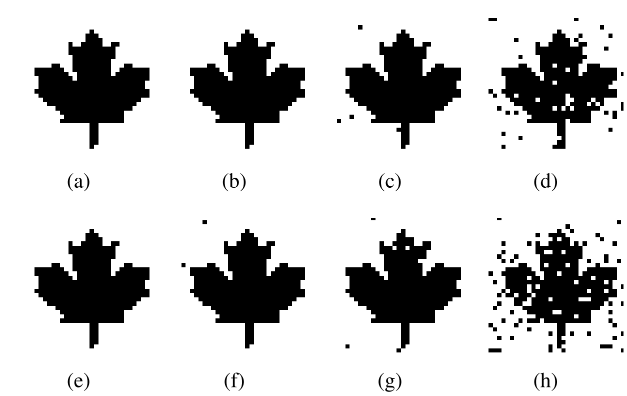

Fig. 9. Extracted watermark logo for watermarked *Lena* image of size 512 × 512 in the presence of different attacks when message length = 1024 bits. (a) Original watermark. (b) With no attack, NC = 1. (c) JPEG QF = 10 and NC = 0.9970. (d) AWGN $\sigma_n = 20$ and NC = 0.9627. (e) Salt and pepper $p = 0.05$ and NC = 0.9985. (f) Median filtering 3 × 3, NC = 1. (g) Rotation $\theta = 0.5°$ and NC = 0.9940. (h) Gamma correction $\gamma = 0.9$ and NC = 0.9296.

length 1024 bits obtained using the proposed method is 39.93 dB, which is higher than 38.03 dB provided by the scheme in [23] and 33.60 dB provided by the scheme in [24], showing a higher imperceptibility of the proposed watermarking scheme.

D. Embedding Meaningful Message

In this section, a meaningful message, e.g., a logo, is chosen as a watermark. In this experiment, a binary logo of size 32 × 32 pixels is inserted in the original image. In order to compare the extracted watermark $\hat{b}$ with the original watermark logo b, the normalized correlation (NC) given by [41], [42]

$$\text{NC} = \frac{\sum_{k=1}^{N_B} b_k \hat{b_k}}{\sqrt{\sum_{k=1}^{N_B} b_k^2}\sqrt{\sum_{k=1}^{N_B} \hat{b_k^2}}} \tag{17}$$

is used. Fig. 9 shows the original watermark as well as the extracted ones when the watermarked *Lena* image undergoes JPEG compression with QF = 10, additive Gaussian noise corruption with $\sigma_n = 20$, salt and pepper noise contamination with $p = 0.05$, median filtering 3 × 3, rotation with $\theta = 0.5°$, and gamma correction with $\gamma = 0.9$. The NC values are also compared in Fig. 9. It is obvious from the results of Fig. 9 that the proposed decoder has a good performance in extracting watermark logo in the presence of various attacks.

V. CONCLUSION

The vector-based HMM has proven to be a powerful statistical model for the wavelet coefficients of images, in view of the fact that it takes into account not only the heavy-tailed characteristic of these coefficients but also the inter-scale and cross-orientation dependencies between them. A robust blind multiplicative watermark decoder has been proposed in this paper, using the vector-based HMM in the wavelet domain. The decoder has been designed using the maximum likelihood criterion. A closed-form expression for the BER for the proposed decoder has been derived and validated experimentally through Monte Carlo simulations using a large set of test images. The performance of the proposed watermark decoder has been studied in detail by conducting several experiments and comparing the results with that of the other existing decoders. It has been shown that the proposed decoder provides a better performance, as its BER is lower than that provided by decoders using Cauchy and GG distributions. The robustness of the proposed watermarking scheme against different attacks, such as JPEG compression, additive Gaussian noise, salt and pepper noise, median filtering, rotation and gamma correction, has been studied, and shown to be more robust than that of the other existing schemes.

REFERENCES

[1] T. Zong, Y. Xiang, I. Natgunanathan, S. Guo, W. Zhou, and G. Beliakov, “Robust histogram shape-based method for image watermarking,” *IEEE Trans. Circuits Syst. Video Technol.*, vol. 25, no. 3, pp. 717–729, May 2015.

[2] G. C. Langelaar, I. Setyawan, and R. L. Lagendijk, “Watermarking digital image and video data. A state-of-the-art overview,” *IEEE Signal Process. Mag.*, vol. 17, no. 5, pp. 20–46, Sep. 2000.

[3] V. R. Doncel, N. Nikolaidis, and I. Pitas, “An optimal detector structure for the Fourier descriptors domain watermarking of 2D vector graphics,” *IEEE Trans. Vis. Comput. Graphics*, vol. 13, no. 5, pp. 851–863, Sep./Oct. 2007.

[4] M. Barni, F. Bartolini, A. De Rosa, and A. Piva, “A new decoder for the optimum recovery of nonadditive watermarks,” *IEEE Trans. Image Process.*, vol. 10, no. 5, pp. 755–766, May 2001.

[5] J. R. Hernandez, M. Amado, and F. Perez-Gonzalez, “DCT-domain watermarking techniques for still images: Detector performance analysis and a new structure,” *IEEE Trans. Image Process.*, vol. 9, no. 1, pp. 55–68, Jan. 2000.

[6] A. Briassouli and M. G. Strintzis, “Locally optimum nonlinearities for DCT watermark detection,” *IEEE Trans. Image Process.*, vol. 13, no. 12, pp. 1604–1617, Dec. 2004.

[7] I. J. Cox, J. Kilian, F. T. Leighton, and T. Shamoon, "Secure spread spectrum watermarking for multimedia," *IEEE Trans. Image Process.*, vol. 6, no. 12, pp. 1673–1687, Dec. 1997.

[8] S. M. M. Rahman, M. O. Ahmad, and M. N. S. Swamy, "A new statistical detector for DWT-based additive image watermarking using the Gauss–Hermite expansion," *IEEE Trans. Image Process.*, vol. 18, no. 8, pp. 1782–1796, Aug. 2009.

[9] Y. Bian and S. Liang, "Locally optimal detection of image watermarks in the wavelet domain using Bessel K form distribution," *IEEE Trans. Image Process.*, vol. 22, no. 6, pp. 2372–2384, Jun. 2013.

[10] R. Kwitt, P. Meerwald, and A. Uhl, "Lightweight detection of additive watermarking in the DWT-domain," *IEEE Trans. Image Process.*, vol. 20, no. 2, pp. 474–484, Feb. 2011.

[11] M. Amini, M. O. Ahmad, and M. N. S. Swamy, "A new blind wavelet domain watermark detector using hidden Markov model," in *Proc. IEEE Int. Symp. Circuits Syst. (ISCAS)*, Jun. 2014, pp. 2285–2288.

[12] M. Amini, M. O. Ahmad, and M. N. S. Swamy, "A new locally-optimum watermark detector in wavelet domain using vector-based hidden Markov model," *Signal Process.*, under review.

[13] Y. Wang, J. F. Doherty, and R. E. Van Dyck, "A wavelet-based watermarking algorithm for ownership verification of digital images," *IEEE Trans. Image Process.*, vol. 11, no. 2, pp. 77–88, Feb. 2002.

[14] H. Sadreazami, M. O. Ahmad, and M. N. S. Swamy, "Multiplicative watermark decoder in contourlet domain using the normal inverse Gaussian distribution," *IEEE Trans. Multimedia*, vol. 18, no. 2, pp. 196–207, Feb. 2016.

[15] E. Nezhadarya, Z. Wang, and R. K. Ward, "Robust image watermarking based on multiscale gradient direction quantization," *IEEE Trans. Inf. Forensics Security*, vol. 6, no. 4, pp. 1200–1213, Dec. 2011.

[16] N. K. Kalantari and S. M. Ahadi, "A logarithmic quantization index modulation for perceptually better data hiding," *IEEE Trans. Image Process.*, vol. 19, no. 6, pp. 1504–1517, Jun. 2010.

[17] M. A. Akhaee, S. M. E. Sahraeian, B. Sankur, and F. Marvasti, "Robust scaling-based image watermarking using maximum-likelihood decoder with optimum strength factor," *IEEE Trans. Multimedia*, vol. 11, no. 5, pp. 822–833, Aug. 2009.

[18] Q. Cheng and T. S. Huang, "An additive approach to transform-domain information hiding and optimum detection structure," *IEEE Trans. Multimedia*, vol. 3, no. 3, pp. 273–284, Sep. 2001.

[19] K. Zebbiche and F. Khelifi, "Efficient wavelet-based perceptual watermark masking for robust fingerprint image watermarking," *IET Image Process.*, vol. 8, no. 1, pp. 23–32, Jan. 2014.

[20] N. Bi, Q. Sun, D. Huang, Z. Yang, and J. Huang, "Robust image watermarking based on multiband wavelets and empirical mode decomposition," *IEEE Trans. Image Process.*, vol. 16, no. 8, pp. 1956–1966, Aug. 2007.

[21] R. Zhang, J. Ni, and J. Huang, "An adaptive image watermarking algorithm based on HMM in wavelet domain," *Acta Autom. Sin.*, vol. 31, no. 5, pp. 705–712, 2005.

[22] J. Ni, J. Zhang, J. Huang, and C. Wang, "A robust multi-bit image watermarking algorithm based on HMM in wavelet domain," in *Proc. Int. Workshop Digit. Watermarking*, 2005, pp. 110–123.

[23] C. Wang, J. Ni, and J. Huang, "An informed watermarking scheme using hidden Markov model in the wavelet domain," *IEEE Trans. Inf. Forensics Security*, vol. 7, no. 3, pp. 853–867, Jun. 2012.

[24] C. Wang, "An enhanced informed watermarking scheme using the posterior hidden Markov model," *Sci. World J.*, vol. 2014, Jan. 2014, Art. no. 345892.

[25] H. Sadreazami and M. Amini, "A robust spread spectrum based image watermarking in ridgelet domain," *AEU-Int. J. Electron. Commun.*, vol. 66, no. 5, pp. 364–371, 2012.

[26] N. K. Kalantari, S. M. Ahadi, and M. Vafadust, "A robust image watermarking in the ridgelet domain using universally optimum decoder," *IEEE Trans. Circuits Syst. Video Technol.*, vol. 20, no. 3, pp. 396–406, Mar. 2010.

[27] H. Sadreazami, M. O. Ahmad, and M. N. S. Swamy, "A study of multiplicative watermark detection in the contourlet domain using alpha-stable distributions," *IEEE Trans. Image Process.*, vol. 23, no. 10, pp. 4348–4360, Oct. 2014.

[28] M. A. Akhaee, S. M. E. Sahraeian, and F. Marvasti, "Contourlet-based image watermarking using optimum detector in a noisy environment," *IEEE Trans. Image Process.*, vol. 19, no. 4, pp. 967–980, Apr. 2010.

[29] H. Sadreazami, M. O. Ahmad, and M. N. S. Swamy, "A robust multiplicative watermark detector for color images in sparse domain," *IEEE Trans. Circuits Syst. II, Express Briefs*, vol. 62, no. 12, pp. 1159–1163, Dec. 2015.

[30] H. Sadreazami, M. O. Ahmad, and M. N. S. Swamy, "Optimum multiplicative watermark detector in contourlet domain using the normal inverse Gaussian distribution," in *Proc. IEEE Int. Symp. Circuits Syst. (ISCAS)*, May 2015, pp. 1050–1053.

[31] H. Sadreazami and M. Amini, "Dual wavelet watermarking using principal component analysis," in *Proc. IEEE Int. Conf. Signal Process. (ICSP)*, Oct. 2010, pp. 1821–1824.

[32] Q. Cheng and T. S. Huang, "Robust optimum detection of transform domain multiplicative watermarks," *IEEE Trans. Signal Process.*, vol. 51, no. 4, pp. 906–924, Apr. 2003.

[33] B. Chen and G. W. Wornell, "Quantization index modulation: A class of provably good methods for digital watermarking and information embedding," *IEEE Trans. Inf. Theory*, vol. 47, no. 4, pp. 1423–1443, May 2001.

[34] S.-C. Pei and J.-H. Chen, "Robustness enhancement for noncentric quantization-based image watermarking," *IEEE Trans. Circuits Syst. Video Technol.*, vol. 16, no. 12, pp. 1507–1518, Dec. 2006.

[35] M. R. Luettgen, W. C. Karl, A. S. Willsky, and R. R. Tenney, "Multiscale representations of Markov random fields," *IEEE Trans. Signal Process.*, vol. 41, no. 12, pp. 3377–3396, Dec. 1993.

[36] M. S. Crouse, R. D. Nowak, and R. G. Baraniuk, "Wavelet-based statistical signal processing using hidden Markov models," *IEEE Trans. Signal Process.*, vol. 46, no. 4, pp. 886–902, Apr. 1998.

[37] M. N. Do and M. Vetterli, "Rotation invariant texture characterization and retrieval using steerable wavelet-domain hidden Markov models," *IEEE Trans. Multimedia*, vol. 4, no. 4, pp. 517–527, Dec. 2002.

[38] M. Amini, M. O. Ahmad, and M. N. S. Swamy, "Image denoising in wavelet domain using the vector-based hidden Markov model," in *Proc. IEEE Int. Conf. New Circuits Syst. (NEWCAS)*, Jun. 2014, pp. 29–32.

[39] M. Amini, M. O. Ahmad, and M. N. S. Swamy, "A new map estimator for wavelet domain image denoising using vector-based hidden Markov model," in *Proc. IEEE Int. Symp. Circuits Syst. (ISCAS)*, May 2015, pp. 445–448.

[40] Online Image Database. [Online]. Available: http://decsai.ugr.es/cvg/dbimagenes/index.php, accessed on Mar. 2013.

[41] H. Sadreazami and M. Amini, "Highly robust image watermarking in contourlet domain using singular value decomposition," in *Proc. IEEE Int. Conf. Signal Process. (ICSP)*, Oct. 2012, pp. 628–631.

[42] M. Amini, K. Yaghmaie, and H. Sadreazami, "A new scheme for dual watermarking using DWT-PCA technique," in *Proc. Int. Conf. Imag. Theory Appl. (IMAGAPP)*, 2010, pp. 43–46.

Marzieh Amini (S'13) received the B.Sc. degree in electrical engineering from K. N. Toosi University of Technology, Tehran, Iran, in 2007 and the M.Sc. degree in electrical engineering from Semnan University, Semnan, Iran, in 2011. She is currently working toward the Ph.D. degree in electrical and computer engineering with Concordia University, Montreal, QC, Canada.

She has been a Research Associate with the Signal Processing Group, Concordia University, since 2011, where she has been involved in statistical image modeling in frequency domains with applications in watermarking and denoising.

Ms. Amini has served as a Reviewer of several journals and major conferences.

M. Omair Ahmad (S'69–M'78–SM'83–F'01) received the B.Eng. degree in electrical engineering from Sir George Williams University, Montreal, QC, Canada, and the Ph.D. degree in electrical engineering from Concordia University, Montreal.

From 1978 to 1979, he was a Faculty Member with New York University, Buffalo, NY, USA. In 1979, he joined the Faculty of Concordia University as an Assistant Professor of Computer Science. He then moved to the Department of Electrical and Computer Engineering, Concordia University, where he is currently a Professor. He was a Founding Researcher with Micronet, Ottawa, ON, Canada, from its inception in 1990 as a Canadian Network of Centers of Excellence to its expiration in 2004. He was an Examiner of the order of Engineers of Quebec. He has authored extensively in the area of signal processing. He holds four patents. His research interests include multidimensional filter design, speech, image and video processing, nonlinear signal processing, communication DSP, artificial neural networks, and VLSI circuits for signal processing.

Dr. Ahmad was a member of the Admission and Advancement Committee of the IEEE in 1988. He is a recipient of numerous honors and awards, including the Wighton Fellowship from the Sandford Fleming Foundation, an induction to Provosts Circle of Distinction for Career Achievements, and the Award of Excellence in Doctoral Supervision from the Faculty of Engineering and Computer Science, Concordia University. He was an Associate Editor of IEEE TRANSACTIONS ON CIRCUITS AND SYSTEMS PART I: FUNDAMENTAL THEORY AND APPLICATIONS from 1999 to 2001. He was the Local Arrangements Chairman of the 1984 IEEE International Symposium on Circuits and Systems. He has served as the Program Co-Chair for the 1995 IEEE International Conference on Neural Networks and Signal Processing, the 2003 IEEE International Conference on Neural Networks and Signal Processing, and the 2004 IEEE International Midwest Symposium on Circuits and Systems. He was a General Co-Chair for the 2008 IEEE International Conference on Neural Networks and Signal Processing. He is the Chair of the Montreal Chapter IEEE Circuits and Systems Society. He was the Chair with the Department of Electrical and Computer Engineering, Concordia University, from 2002 to 2005. He holds the Concordia University Research Chair (Tier I) in Multimedia Signal Processing.

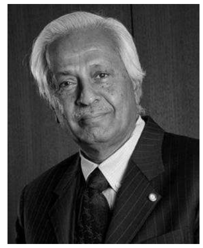

M.N.S. Swamy (S'59–M'62–SM'74–F'80) received the B.Sc. (Hons.) degree in mathematics from Mysore University, Mysore, India, in 1954, the Diploma degree in electrical communication engineering from the Indian Institute of Science, Bangalore, India, in 1957, and the M.Sc. and Ph.D. degrees in electrical engineering from the University of Saskatchewan, Saskatoon, SK, Canada, in 1960 and 1963, respectively.

He was conferred the title of Honorary Professor at National Chiao Tong University, Hsinchu, Taiwan, in 2009. He is currently a Research Professor in the Department of Electrical and Computer Engineering, Concordia University, Montreal, QC, Canada, where he served as the Founding Chair of the Department of Electrical Engineering from 1970 to 1977, and Dean of Engineering and Computer Science from 1977 to 1993. Since July 2001, he has held the Concordia Chair (Tier I) in Signal Processing. He has also taught in the Electrical Engineering Department, Technical University of Nova Scotia, Halifax, NS, Canada, and the University of Calgary, Calgary, AB, Canada, as well as in the Department of Mathematics, University of Saskatchewan. He was a founding member of Micronet, Ottawa, ON, Canada, from its inception in 1990 as a Canadian Network of Centers of Excellence until its expiration in 2004, and was also its Coordinator for Concordia University. He has coauthored six books and three book chapters. He holds five patents. His research interests include number theory, circuits, systems and signal processing.

Dr. Swamy is a Fellow of the Institute of Electrical Engineers (U.K.), the Engineering Institute of Canada, the Institution of Engineers (India), and the Institution of Electronic and Telecommunication Engineers (India). In 2008, Concordia University instituted the M. N. S. Swamy Research Chair in Electrical Engineering as recognition of his research contributions. In 2009 he was inducted to the Provosts Circle of Distinction for career achievements. He has served the IEEE in various capacities such as the President-Elect in 2003, President in 2004, Past-President in 2005, Vice President (Publications) during 2001–2002, Vice-President in 1976, Editor-in-Chief of the IEEE TRANSACTIONS ON CIRCUITS AND SYSTEMS—I: FUNDAMENTAL THEORY AND APPLICATIONS from June 1999 to December 2001, Associate Editor of the IEEE TRANSACTIONS ON CIRCUITS AND SYSTEMS from June 1985 to May 1987, Program Chair for the 1973 IEEE CAS Symposium, General Chair for the 1984 IEEE CAS Symposium, Vice-Chair for the 1999 IEEE Circuits and Systems (CAS) Symposium, and a member of the Board of Governors of the CAS Society. He was the recipient of many IEEE CAS Society awards, including the Education Award in 2000, the Golden Jubilee Medal in 2000, and the 1986 Guillemin-Cauer Best Paper Award. He has been the Editor-in-Chief of Circuits, Systems, and Signal Processing (CSSP) since 1999. Recently, CSSP has instituted a Best Paper Award in his name.